Available online at www.sciencedirect.com

Resuscitation Plus

journal homepage: www.journals.elsevier.com/resuscitation-plus

Experimental paper

MLWAVE: A novel algorithm to classify primary versus secondary asphyxia-associated ventricular fibrillation

Dieter Bender[a,*], *Ryan W. Morgan*[b], *Vinay M. Nadkarni*[b], *Robert A. Berg*[b], *Bingqing Zhang*[c], *Todd J. Kilbaugh*[b], *Robert M. Sutton*[b], *C. Nataraj*[d]

[a] *Villanova Center for Analytics of Dynamic Systems, Villanova University, Villanova, PA, USA*

[b] *Department of Anesthesiology and Critical Care Medicine, The Children's Hospital of Philadelphia, University of Pennsylvania, Philadelphia, PA, USA*

[c] *Healthcare Analytics Unit, Department of Biomedical and Health Informatics, The Children's Hospital of Philadelphia, Philadelphia, PA, USA*

[d] *Moritz Professor & Director, Villanova Center for Analytics of Dynamic Systems, Villanova University, Villanova, PA, USA*

Abstract

Introduction/Hypothesis: The outcome of cardiopulmonary resuscitation (CPR) depends on timely recognition of the underlying cause of cardiac arrest. Ventricular fibrillation (VF) waveform analysis to differentiate primary VF from secondary asphyxia-associated VF may allow tailoring of therapies to improve cardiac arrest outcomes. Therefore, the primary goal of this investigation was to develop a novel technique utilizing wavelet synchrosqueezed transform (WSST) and decision-tree classifier that was specifically adapted to discriminate between these two incidents of VF.

Methods: Secondary analytical investigation of electrocardiography (ECG) data obtained from swine models of either primary VF (n=18) or secondary asphyxia-associated VF (7 min of asphyxia prior to VF induction; n=12). In the primary analysis, WSST technique was applied to the first 35 s of the VF ECG signal to identify the most differentiating characteristics of the signal for use as features to develop a machine learning algorithm to classify the arrest as either primary VF vs. secondary asphyxia-associated VF. The performance of this new interactive Machine Learning algorithm with Wavelet Energy features of ECG (MLWAVE) was assessed using both classification accuracy and area under the receiver operating characteristic curve (AUCROC). To evaluate the validity of the new technique, the amplitude spectrum area (AMSA)-based technique, a well-established defibrillation classification method, was also applied to the same ECG signals. The classification accuracy and AUCROC were then compared between the two techniques.

Results: For the primary analysis evaluating the first 35 s of the VF waveform, the MLWAVE technique classified the type of VF with high accuracy (28/28 [100%], AUCROC: 1.00). The MLWAVE technique performed better than the AMSA technique across all comparisons, but given the small sample sizes, differences were not statistically significant (accuracy: 100% vs. 85.7%; p=0.24; AUCROC: 1.00 vs. 0.82; p=0.24).

Conclusion: This analytical investigation illustrates the advantages of the MLWAVE signal processing method which was associated with 100% accuracy in classifying the type of VF waveform: primary vs. asphyxia-associated. Such classification could lead to personalized tailoring of resuscitation (e.g., immediate defibrillation vs. continued CPR and treatment of reversible cardiac arrest causes before defibrillation) to improve outcomes for cardiac arrest.

Keywords: Electrocardiography, Wavelet transform, Cardiac arrest, Cardiopulmonary resuscitation, Ventricular fibrillation, Asphyxia

* Corresponding author at: Villanova University, Villanova Center for Analytics of Dynamic Systems, 800 E. Lancaster Ave., Villanova, PA 19085, USA.
E-mail address: dbender2@villanova.edu (D. Bender).

http://dx.doi.org/10.1016/j.resplu.2020.100052
Received 18 August 2020; Received in revised form 8 November 2020; Accepted 10 November 2020

Introduction

Cardiac arrest (CA) is an important public health problem. Despite improving survival rates over the past 20 years, most patients still do not survive; among survivors, many suffer life-limiting neurological injury.[1,2] Personalized resuscitation has been highlighted as a potential therapeutic strategy to improve outcomes further, but implementation has been limited due to a lack of clinical tools to allow prompt identification of underlying pathophysiologic states.[3,4]

Ventricular fibrillation (VF) is a cardiac arrest, characterized as rapid, disorganized contractions of the heart with complex electrocardiogram (ECG). To that end, quantitative analysis of the VF waveform holds promise as a potential tool to improve personalization of resuscitation technique. Measurable quantitative features such as amplitude and frequency have been associated with defibrillation success, short-term, and long-term outcomes.[5–7] Because these quantitative measures are indicative of the metabolic state of the heart, they may help a rescuer personalize which therapies are likely to provide the most immediate benefit (i.e., cardiopulmonary resuscitation [CPR] vs. medications vs. prompt de- fibrillation). Because VF occurs at some point in more than 20% of pediatric and more than 40% of adult resuscitations,[8] these analytic methods have the potential to improve the care provided to a substantial proportion of CA patients.

Despite promising applications of existing VF waveform analytic methods (e.g., AMSA: amplitude spectral area), certain analytic characteristics limit its value. For example, time-sensitive frequency trends that might contribute valuable information about the signal remain uncaptured. This drawback derives from the mathematical limitations of the fast Fourier transform (FFT), which is the basis for calculating AMSA value of a VF waveform. In contrast, wavelet transform (WT) provides an elegant mathematical solution that addresses FFT limitations, presenting more quantifying information of the waveform. As such, the objective of this study was to determine if an optimal synthesis of new WT analysis and machine learning (ML) could discriminate between primary and secondary asphyxia-associated VF. Since AMSA values are often used to quantify VF type[9,10] as frequently reported in literature, e.g., Indik et al.[5–7,11,12] and Bonnes et al.,[13–15] we adopted their ECG metrics and methodology to validate our method.

Methods

Animal data

In this retrospective analysis, the data was taken from 30 healthy 3-month-old female domestic swine with two different conditions introduced during the experiment. Group A: primary normoxic VF (n=18) and Group B: secondary asphyxia-associated VF (n=12). In Group A, VF was induced by electrical pacing, and after confirmation of VF, the animal remained untreated for 7 min. In Group *B*, after asphyxia was administered through endotracheal tube clamping for 7 min, to ensure a standard length of asphyxia (7 min), VF was immediately induced electrically (<10 s) using a bipolar pacing catheter that was advanced into the right ventricle. Following the injury period of 7 min, CPR was provided for both groups with a target rate of 100 chest compressions (CC) per minute (CC/min) and ventilations at 6 min-1 with 100% oxygen. Due to the nature of original experiments,[16,17] half of the animals from each group randomly received either hemodynamic-directed CPR (HD-CPR), consisting of compression depth titrated to a target systolic blood pressure of 100 mmHg; or optimal American Heart Association Guideline care (Guideline-care), consisting of target depth of 51 mm and epinephrine every four minutes.[18,19] However, no intravenous vasopressors were administered in HD-CPR nor the Guideline-care in the first 2 min of provided CPR. The experimental protocol[16,17] was approved by The Children's Hospital of Philadelphia Institutional Animal Care and Use Committee, as previously described in Refs.[16,17] As cited above, this is a retrospective analysis of the data acquired for hemodynamic-directed CPR studies[16,17] and, therefore, introduces some limitations to this study's design. One of them is that two samples (one from each group) did not have full recordings of the ECG waveforms during the 7 min injury period. This resulted in $N = 28$ samples (instead of $N = 30$) for the A and B comparisons.

Algorithm development

Overview

The ECG waveform was sampled at different locations to address the primary and secondary goals of this study. The primary objective was to differentiate between immediate normoxic VF and immediate asphyxia-associated VF. Here we examined the comparison between the waveforms during time-intervals [A_1, A_2; 35-second sample] and [B_1, B_2; 5-second sample], as illustrated in Fig. 1. In addition, we also analyzed the waveforms during time-intervals [C_1, C_2; 5-second sample], a period where both types of VF had been treated with 30 s of CPR (i.e., the only difference between the conditions was untreated VF versus asphyxia prior to initiation of CPR).

Although there currently exists no specific method to differentiate between the two CA pathologies solely using the ECG signal, to investigate the accuracy of the developed MLWAVE (Machine Learning Algorithm with Wavelet Energy features of ECG) technique, AMSA, a well-established method to predict defibrillation outcome was adapted to address this problem in order to compare to and evaluate the results of our new technique.

Waveform analysis

The first step of the technique was to identify relevant frequency characteristics in the ECG signals to ultimately utilize them as input data to a ML classification algorithm. The examination of the frequency content was carried out through WT. As shown through previous studies,[20,21] WT provides extraordinary insights regarding frequencies and their attributes often hidden in the raw ECG signal with respect to their temporal locations. This ability is of particular interest when the analyzed waveforms such as ECG (unlike sound waves) are transient and non-stationary, meaning that the waveforms content has time specific discontinuities and breakdown points or trends and transients that might be profoundly meaningful. Mathematically, one can interpret the result of the WT, $W_1(s, \mu)$), as a frequency power spectrum with a time vector and the transform is described mathematically by Eqn. 1.

$$W\{fs,\mu)\} = f, \Psi_{s,\mu}) = \int_{-\infty}^{\infty} f(t)\Psi_{s,\mu}(t)dt = \int_{-\infty}^{\infty} f(t)\frac{1}{\sqrt{|s|}}\Psi^{*}\left(\frac{t-\mu}{s}\right)dt, \quad (1)$$

where, in our case, the continuous signal $f(t)$ = ECG is cross correlated with the Morlet wavelets ($\Psi s,\mu$) of different widths defined by the s parameter and at different temporal locations along the time axis governed by the translational parameter μ.

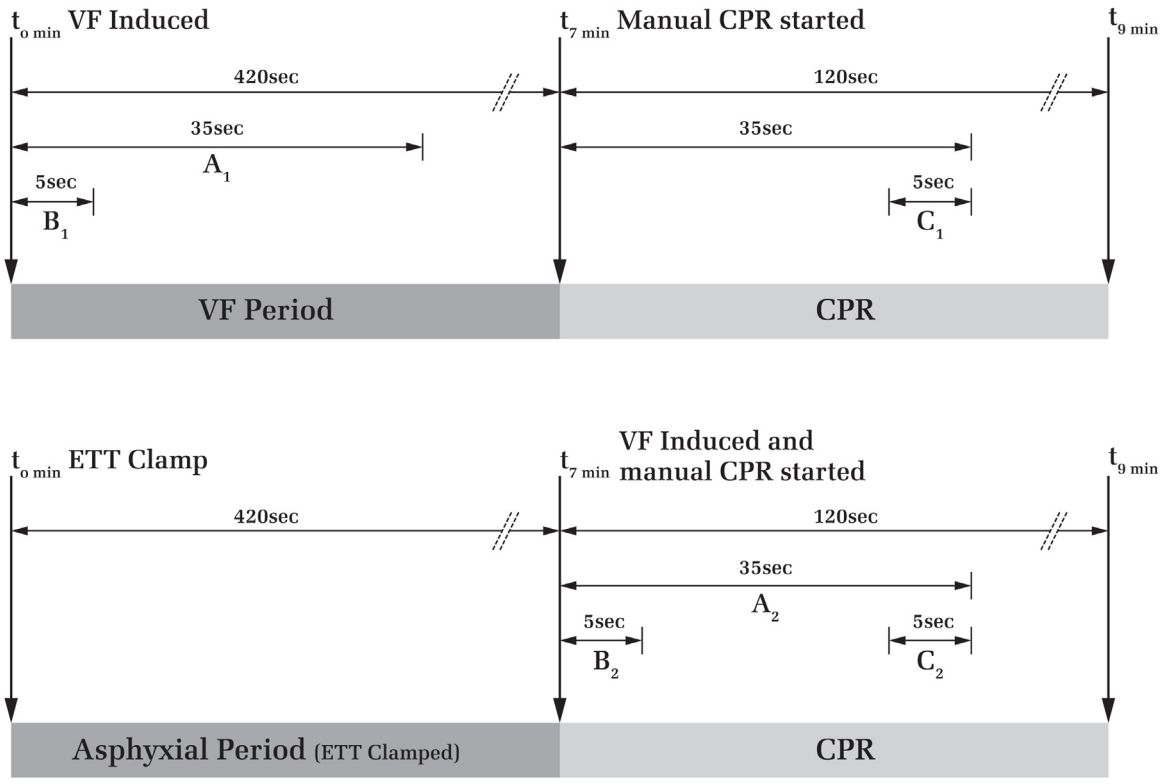

Fig. 1 – Evaluation Protocol; ETT, endotracheal tube; VF, ventricular fibrillation; CPR, cardiopulmonary resuscitation.

The preliminary investigation of this work[21] suggested that frequency modes and trends with respect to time within the ECG signal could be of high importance for this analysis. However, due to the nature of traditional wavelet transform, frequency trends on the time-frequency plane are captured in a somewhat continuous representation; the effect is often referred to as energy smearing and is illustrated in Fig. 2b. As a result, to analyze the frequency modes and frequency trends embedded in the raw ECG signal in a much more precise way with respect to time, we adopted a modified operator called wavelet synchrosqueezed transform (WSST). As shown through graphical representation in Fig. 2c, this type of transform provides a more detailed time-frequency representation from which instantaneous frequency trends can be extracted more accurately.[20,22–25]

Knowing that CC were performed at a rate of 1.6*Hz* (100 CC/min), WSST was performed with two different scale-dependent frequency bands ($B_1 = [1,4]Hz$, $B_2 = [4,17]Hz$) on each ECG waveform to allow for examination of the waveform without CC artifacts separately. A graphical illustration of the separation can be seen in Fig. 2d and 2e for an asphyxia sample. The separation is described mathematically by Eqn. 2, where $f(t) = ECG$, $\Psi_{s,\mu}$ is the mother wavelet with s and μ being the scaling and temporal parameters, respectively. The bandwidth in Eqn. 2 is defined by the scales [s_1, s_2], that are derived from the set bandwidth frequencies [f_1, f_2].

$$W_n\{fs_1 - s_2, \mu)\} = f(t), \Psi_{s_1 - s_2, \mu}) \quad (2)$$

Next, the obtained WSST coefficient spectrum $W_2(f(4, 17Hz, \mu))$ of each ECG segment was quantified numerically with respect to the frequency and time-frequency domains, summarizing the characteristics of each ECG signal for the ML algorithm. These steps are illustrated in Fig. 3 for a normoxic VF and an asphyxia-associated VF sample. To obtain the characteristics from each WSST coefficient spectrum with respect to the frequency domain, the energy $E_i(s_i)$ was calculated with respect to each frequency (scale) according to Eqn. 3. This provided a frequency function shown in Fig. 3c, describing the frequency content in the ECG signal unique to every ECG segment. The energy function was described through the magnitude of the most dominant frequency ($|E(s)|_{max}$) and the average frequency-bandwidth energy, yielding the first two characteristic features for each individual sample.

$$E_i s) = |W_i\{fs_i, \mu)\}|^2 \quad (3)$$

In the following step, the frequency content was explored in the time-frequency domain to quantify frequency trends in each signal. Here, the idea was to look at the distribution of the most dominant frequencies with respect to time. We defined the most dominant frequencies as the magnitude peaks on the time-frequency plane, as they appear in Fig. 3d. Since the frequency modulation was kept to a minimum through a narrow frequency-bandwidth in $W_1\{f(s_{11} - s_{12}, \mu)\}$, the frequency trends were only calculated for the WSST coefficient spectrum $W_2\{f(s_{21} - s_{22}, \mu)\}$. To preserve the overall trend of frequencies with respect to time, a polynomial function Eqn. 4 was fitted to the scattered locations of the peaks in the time-frequency plane. Next, the distribution of the peaks was quantified in the form of perpendicular distance from the fitted curve to the location of each peak. Fig. 3d illustrates this process in a more geometrical representation for one of the frequency peaks.

$$yt) = at^2 + bt + c \quad (4)$$

Using the calculated distances, statistical values were calculated to summarize the revealed frequency trends in each ECG waveform. This process was repeated for each ECG signal resulting in six

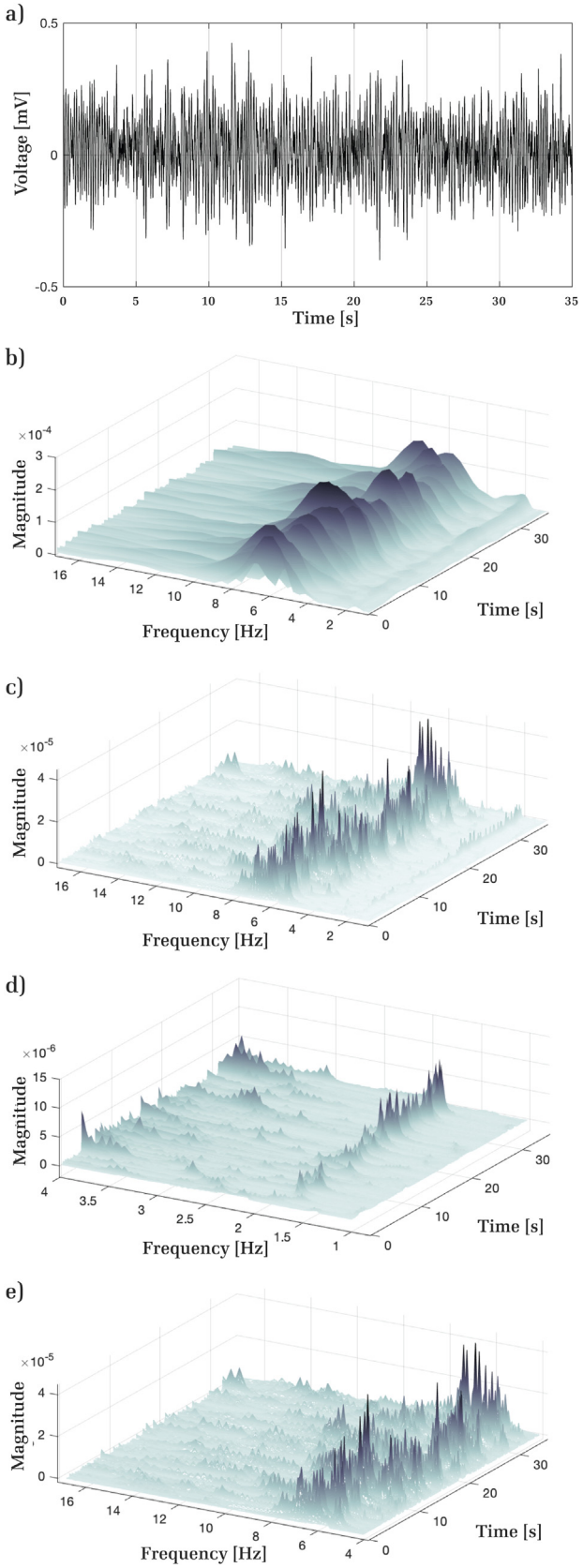

Fig. 2 – a) Original ECG waveform, b) ECG WT coefficient spectrum $W(s,\mu)$ with bandwidth B = [1,17]Hz, c) ECG WSST coefficient spectrum $W_{SST}(s,\mu)$ with bandwidth B = [1,17]Hz, d) WSST coefficient spectrum $W_1 f(s_1 s_2, \mu)$, with bandwidth B_1 = [1,4]Hz, e) WSST coefficient spectrum $W_2 f(s_1 s_2, \mu)$, with bandwidth B_2 = [4,17]Hz; ECG, electrocardiogram; WT, wavelet transform; WSST, wavelet synchrosqueezed transform; B, bandwidth; s, scale; f, frequency; μ, translational parameter.

additional features per signal. Hence, the initial ML classifier was constructed with an input data of 30 samples, each with a set of eight characteristic features: energy (E_2); area under the curve (AUC_2); interquartile range (IQR); median absolute deviation (MAD); central moment of order two (CM_2); range of values (RoV); standard deviation (StD); and, variance (Var).

Machine learning

Since the task at hand is to classify two different pathophysiologic paths of the CA, a binomial coarse decision-tree classifier was selected as the ML model. The learning structure of a decision-tree classifier is driven by an information-gain heuristic and provides an efficient method for finding a simple classification model. If the performance of the decision-tree classifier is decided to be suitable for a given task, the most important characteristics of the signal can be easily identified and improved in terms of their effect on accuracy, generalization, and overfitting of the final classifier.

From the performance of the decision-tree classifier, it was deduced that interquartile range (IQR) and median absolute deviation (MAD) features provide the best possible class separation in the initial classification attempts, as shown in Fig. 4. Since all of these characteristic values depend on a bandwidth of $B_2 = [f_4, f_{17}]$, it was safe to assume that the performance of the classifier depends on the bandwidth as well. Thus, an optimization technique was developed to obtain the best possible bandwidth limits $[f_1, f_2]$. The accuracy of a tree classifier model served as the cost function for the optimization, where the structure of the tree classifier was constrained by the features IQR and MAD, as shown in Fig. 4. The bandwidth limits $[f_1, f_2]$ served as design parameters ranging from $4Hz$ to $20Hz$. The generalized genetic[26] and pattern search[27] optimization techniques were used to obtain the best bandwidth since both methods are relatively robust to local minima and converge reasonably quick to an optimal solution. Both optimization techniques yielded similar results.

Giving that this is retrospective data with some limitations imposed by the original design of the study and small sample size with unknown inter-patient distribution, we have chosen to rely on error minimization and generalization optimization with given samples, instead of extending the data set by synthetic representatives as is often done with non-medical data sets.[26,28] Thus, we address the limited number of samples by using k-fold cross-validation ($k = 8$), a widely employed technique that utilizes all available data for training and evaluation, ensuring the retention of the high generality principle of any ML classifier.

Baseline algorithm

Although there currently exists no specific method to differentiate between the two CA pathophysiologies solely using the ECG signal, AMSA, a well-established method to predict defibrillation outcome was adapted and applied to address this problem to principally serve as a point of comparison to MLWAVE.

Among the different VF waveform parameters, AMSA has demonstrated in multiple observational and retrospective studies the correlation between the AMSA value of the VF ECG signal and the

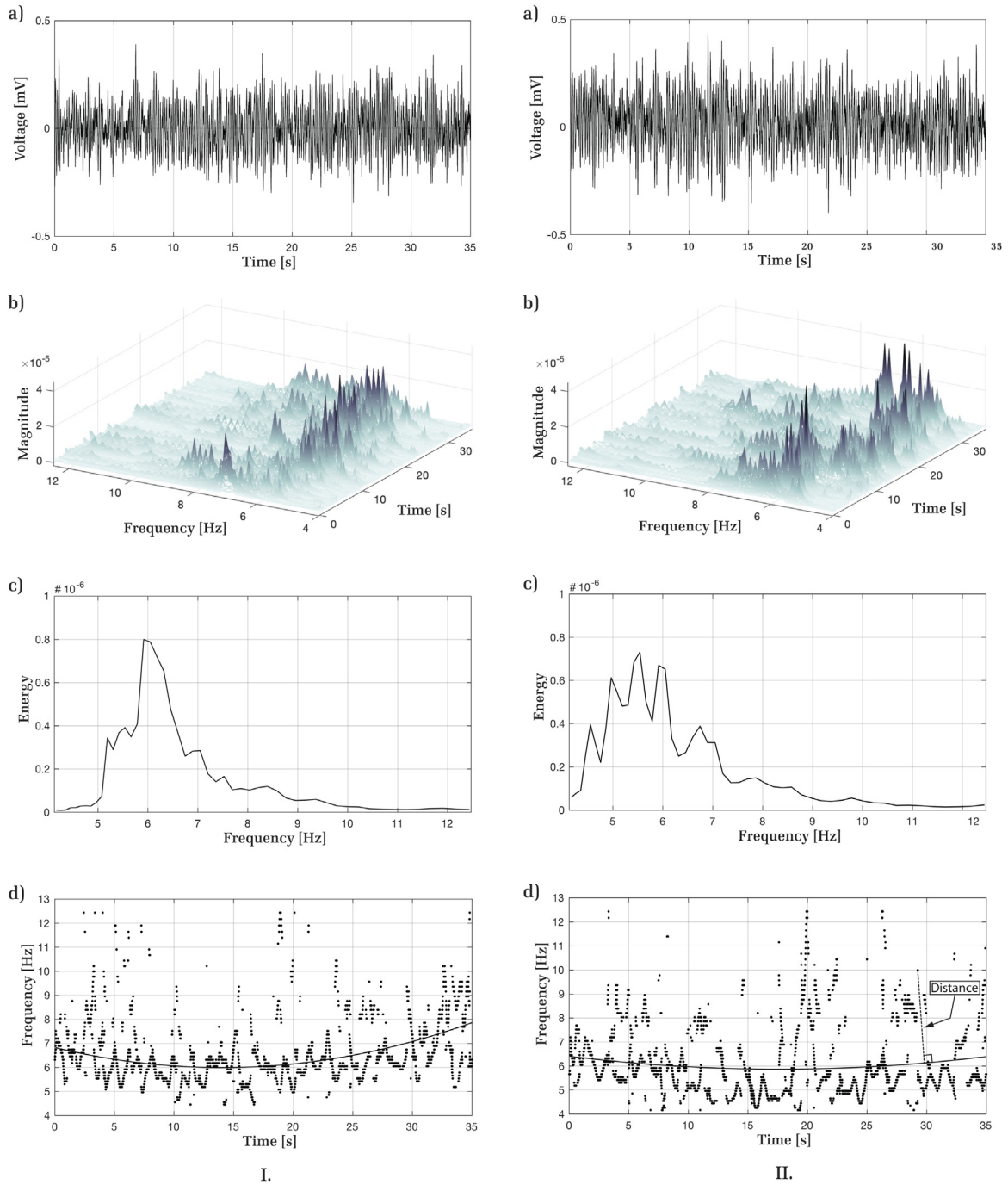

Fig. 3 – I. VF sample and II. Asphyxia sample; a) original ECG waveform, b) ECG WSST coefficient spectrum $W_1 f$([4, 12.5] *Hz*, μ), c) frequency vs. *E*, d) distribution of peaks on the time-frequency plane; VF, ventricular fibrillation; ECG, electrocardiogram; WT, wavelet transform; WSST, wavelet synchrosqueezed transform; E, energy; *f*, frequency; μ, translational parameter.

success of the defibrillation.[29–33] Since the methods including AMSA values are often used to quantify VF type[9,10] as frequently reported in literature[5–7,11–14,34] we have adopted their ECG metrics such as: mean absolute amplitude, AMSA, most dominant frequency, median frequency and interquartile bandwidth range, to validate our method.

Evaluation

The primary points of analysis were during the first 35 s and 5 s, respectively, of the VF waveform in both conditions. (A_1 and A_2, and B_1 and B_2, Fig. 1.). The secondary point was during the 5 s, 30 s after initiation of resuscitation during active chest compressions (C_1 and C_2, Fig. 1). The primary outcome

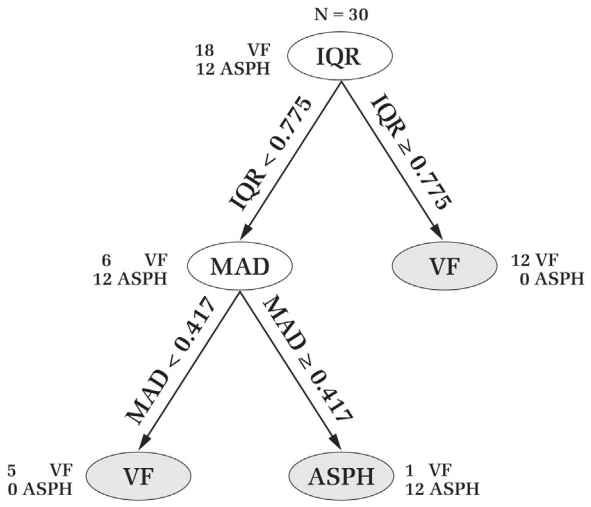

Fig. 4 – Structure of the coarse tree classifier with the most relevant features; VF, ventricular fibrillation; ASPH, asphyxia; IQR, interquartile range; MAD, median absolute deviation.

was classification accuracy defined as: (((*true positives* + *true negatives*)/*number of samples*) 100) of MLWAVE technique. The performance of the MLWAVE technique was compared to the AMSA-based technique using classification accuracy and AUCROC as a measure of class separability. Fisher's exact test was used to compare classification accuracy between the techniques, while DeLong's test to compare the ROC.[35,36] To account for within-subject correlation, Generalized Estimation Equation (GEE) with binary distribution, logit link function and exchangeable working correlation matrix was applied to compare classification accuracy as a sensitivity analysis.

Results

The final MLWAVE classification technique was developed using the 8-dimensional input data from each sample. Fig. 5 summarizes the classification accuracy and AUCROC for MLWAVE and AMSA-based techniques. The result illustrated that MLWAVE outperformed the AMSA-based technique in all comparisons, with a perfect performance in ECG segments [A_1, A_2; 35-second sample] (accuracy: 100% vs. 85.7%; p=0.24, AUCROC: 1.00 vs. 0.82; p=0.24) and a substantial superiority in shorter ECG segments [B_1, B_2; 5-second sample] (accuracy: 92.86% vs. 82.1%; p=0.25, AUCROC: 0.93 vs. 0.86; p=0.13), although the differences were not statistically significant. The MLWAVE also had higher classification accuracy in the [C_1, C_2; 5-second sample] segments, where both VF groups had CPR performed for 30 s, although again, comparisons were not statistically significant (accuracy: 93.3% vs. 83.3%; p=0.42, AUCROC: 0.94 vs. 0.83; p=0.14). The result is consistent with sensitivity analysis.

Discussion

In this study, we used a sophisticated analytical technique to develop an MLWAVE technique to discriminate between primary VF and secondary asphyxia-associated VF with 100% accuracy in approximately 30 s. Such rapid and accurate classification could allow the provider to tailor CPR interventions to etiology of arrest. To our knowledge, the presented approach is the first automated decision support system for this longstanding critical problem.

The high classification accuracy was achieved through complementary interaction of ML and WSST analysis, which revealed several essential and previously unknown characteristics embedded in the ECG waveform. In comparison, the novel MLWAVE technique performed with higher accuracy than the AMSA-based technique.

One of the reasons why MLWAVE outperformed the AMSA-based technique lies in the advantages of the applied WT. Despite many proven applications of AMSA in critical care and particularly in defibrillation technology, the inherent mathematical limitations of AMSA bear several weaknesses. The AMSA value is calculated from the frequency power spectrum obtained through the FFT over a defined time window. The shortcoming of FFT is that it fails to provide any time reference to the frequency content in its spectrum. Any hidden frequency trends, defined as frequency modulation with

COMPARED INTERVALS	AMSA-BASED ALGORITHM			MLWAVE ALGORITHM			p-VALUE	
	AUROC	ACCURACY (%)	CONFUSION MATRIX	AUROC	ACCURACY (%)	CONFUSION MATRIX	AUROC	ACCURACY
A_1 vs. A_2	0.82	85.7	N=28: TRUE VF → PREDICTED VF 16, ASPH 1; TRUE ASPH → PREDICTED VF 3, ASPH 8	1.00	100	N=28: TRUE VF → PREDICTED VF 17, ASPH 0; TRUE ASPH → PREDICTED VF 0, ASPH 11	0.24	0.24
B_1 vs. B_2	0.86	82.1	N=28: TRUE VF → PREDICTED VF 14, ASPH 3; TRUE ASPH → PREDICTED VF 2, ASPH 9	0.93	92.9	N=28: TRUE VF → PREDICTED VF 16, ASPH 1; TRUE ASPH → PREDICTED VF 1, ASPH 10	0.25	0.13
C_1 vs. C_2	0.83	83.3	N=30: TRUE VF → PREDICTED VF 15, ASPH 3; TRUE ASPH → PREDICTED VF 2, ASPH 10	0.94	93.3	N=30: TRUE VF → PREDICTED VF 16, ASPH 2; TRUE ASPH → PREDICTED VF 0, ASPH 12	0.42	0.14

Fig. 5 – Results comparison between the AMSA-based and the developed MLWAVE technique; AMSA, amplitude spectral area; MLWAVE, Machine Learning Algorithm with Wavelet Energy features of ECG; AUCROC, area under the receiver operating characteristic curve; VF, ventricular fibrillation; ASPH, asphyxia; N, number of samples.

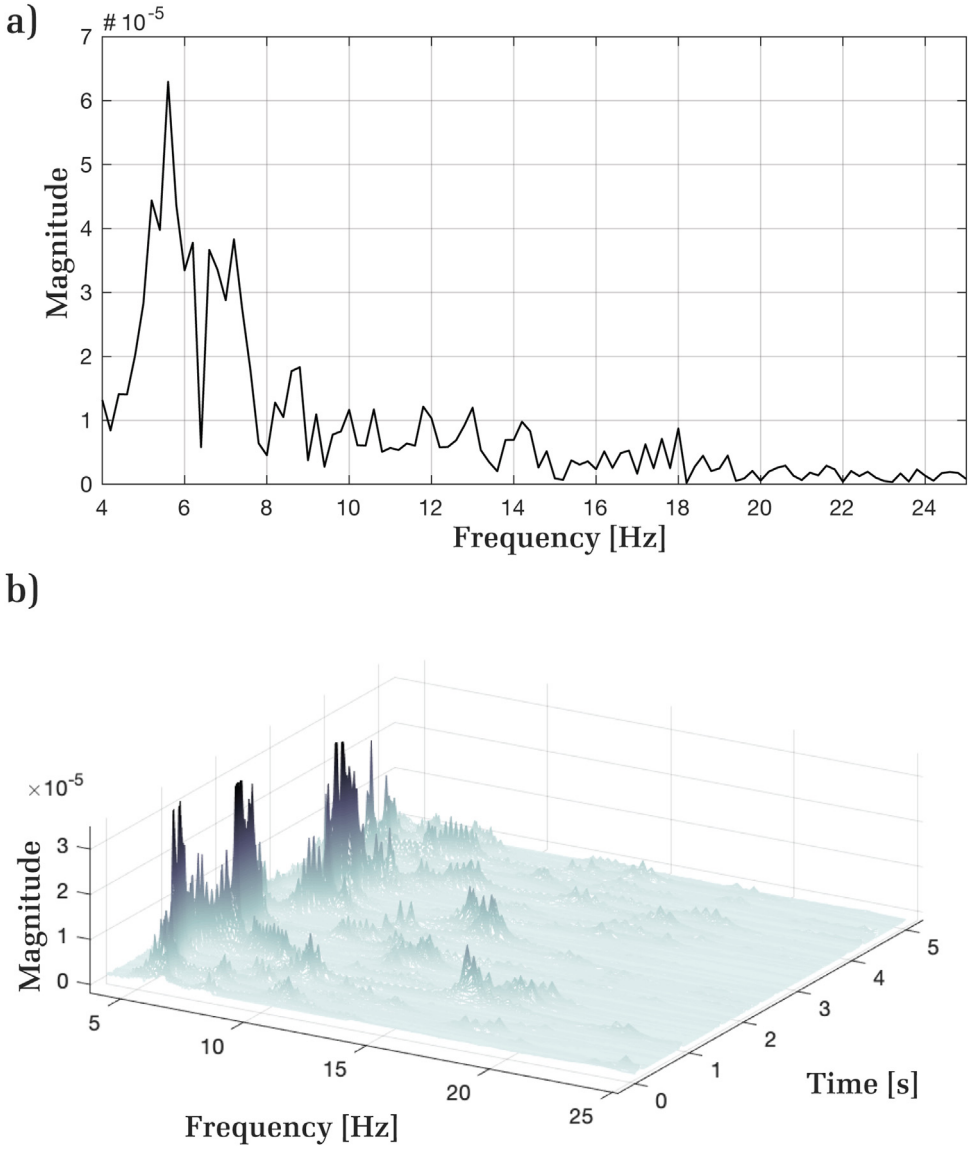

Fig. 6 – a) Fast Fourier transform of a 5s ECG segment that underlines the AMSA approach and b) Wavelet synchrosqueezed transform of the same 5s ECG segment that underlines our approach; ECG, electrocardiogram; AMSA, amplitude spectral area.

respect to time within the ECG signal, remain invisible in the FFT power spectrum (see Fig. 6a). The wavelet transform, as well as the wavelet synchrosqueezed transform, provide an elegant solution to address this drawback by detecting all the time-dependent frequency modulations that remain undetected in the FFT power spectrum (see Fig. 6b).

Although WT applications have appeared in the conventional ECG signal analysis,[20,22,23,37–39] most of the ideas reported in this study had to be reformulated from basic WT concepts to address the VF patterns. First, utilizing computational optimization of the convoluted WSST and ML algorithm, we were able to identify relevant frequency bandwidth to characterize the VF types. The most apparent characteristics separating the VF waveform types were embedded in the frequency bandwidth B=[4, 12.5] Hz of the raw ECG signal. Second, this novel approach provided a way to detect and capture relevant frequency trends. In comparison to the AMSA-based technique, the frequency trends added an amendatory dimension to characterize the VF waveforms, providing a notable advantage to MLWAVE, as reflected in the results of A_1 & A_2 and B_1 & B_2. Comparing specifically the results of the ECG intervals [B_1, B_2; 5-second sample], we showed that even in timely short waveforms, there exists a correlation between the variances of dominant frequencies and the VF types. Furthermore, while one might argue that our selection of A_1 & A_2 and B_1 & B_2 for technique assessment is flawed due to the presence of CPR in A_2 & B_2 and not in A_1 & B_1, the MLWAVE results of ECG intervals as compared in C_1 & C_2 demonstrate that the technique can classify VF with high accuracy even when CPR has been provided for 30s in both conditions and while the intervals C_1 & C_2, demonstrate that the technique can classify VF with high accuracy even when CPR has been provided for 30s in both conditions and while intervals C_1 and C_2 are intrinsically different, due to the prolonged VF injury in the C_1 samples.

The potential clinical relevance of our findings deserve mention. Existing CPR guidelines offer a provider-centric approach that does not necessarily take into account patient factors such as etiology of arrest, intra-arrest physiology, or response to resuscitation. In contrast, there is a growing body of translational and clinical science suggesting that a personalized approach to resuscitation may improve outcomes.[16,17,40–42] With continued refinement, our MLWAVE technique could be used to help a provider tailor the initial resuscitation efforts. For example, patients with asphyxia VF may respond better to defibrillation attempts after providing CPR to restore oxygenation/favorable metabolic milieu rather than immediate defibrillation. Such an approach would be more consistent with a personalized resuscitation approach and could be used to improve CA outcomes.

The possible underlying clinical physiologic mechanisms behind our findings are worthy of comment. It is well known that VF waveform characteristics such as AMSA are indicative of the underlying metabolic substrate of the myocardium (e.g., ATP, ADP) and therefore, the likelihood of defibrillation success.[43] Although completely speculative, it may be that asphyxia prior to VF results in differential substrate availability across varying regions of the heart. Such an occurrence would result in more heterogeneity in the VF frequencies ob- served in these asphyxiated samples.[44] Again, while speculative, this finding of higher variance of VF frequencies have uncovered the need for further clinical study to discover the underlying physiologic mechanism of our ML analyses.

This study has some limitations. First, even though MLWAVE had higher classification accuracy than the AMSA approach for all periods, we were possibly underpowered (due to small sample size) to detect statistically significant differences in this work. Thus, to assure adequate performance on unseen data samples, other ML classifiers, such as Random Forest that achieve the same performance (A_1 vs. A_2 accuracy: 28/28 [100%], AUCROC: 1.00) as the presented Decision-Tree classifier during the development stage but tend to be more robust to overfitting, should be evaluated as an ML classifier in the developed MLWAVE technique. Second, although swine are commonly used for CA models due to their similarities to humans, validation of our method using human clinical data is necessary to establish its relevance to clinical care. Third, our MLWAVE technique cannot provide classification results within the first 5s because it requires a 5s delay for signal analysis. Although immediate determination would be ideal, it is likely that such a short delay would not be clinically important in actual practice. Lastly, since this was a retrospective analysis, prospective validation of the MLWAVE technique is required.

Conclusion

This paper introduces a new method that we call MLWAVE to classify two types of VF arrests, primary normoxic VF and asphyxia-associated VF. Utilizing the detected and previously unknown frequency trends within the ECG waveform, MLWAVE could alert the provider as to whether the event was primary VF versus secondary asphyxia-associated VF with 100% accuracy in a time period of 35s and with 92.9% accuracy in 5s. It should be noted that this is the first documented research project to analyze this critical problem using a non-invasive method, the significance of which could lead to personalized tailoring of resuscitation with the goal to improve outcomes from cardiac arrest.

Conflicts of interest

The authors report no conflicts of interest related specifically to this manuscript. Unrelated disclosures include the following: Robert M. Sutton reports grant funding from the National Institutes of Health (NIH); Vinay M. Nadkarni reports grant funding from NIH, the Agency for Healthcare Research and Quality, Zoll Medical, Nihon-Kohden and the American Heart Association (AHA); Robert A. Berg reports grant funding from NIH; Ryan W. Morgan reports grant funding from NIH; Todd J. Kilbaugh reports grant funding from NIH and the Department of Defense. C. Nataraj reports funding from NIH and ONR.

REFERENCES

1. Holmberg MJ, Ross CE, Fitzmaurice GM, Chan PS, Duval-Arnould J, Grossestreuer AV, et al. Annual incidence of adult and pediatric in-hospital cardiac arrest in the United States. Circulation: Cardiovascular Quality and Outcomes 2019;12(7):e005580.
2. Berg RA, Nadkarni VM, Clark AE, Moler F, Meert K, Harrison RE, et al. Incidence and outcomes of cardiopulmonary resuscitation in PICUs. Critical care medicine 2016;44(4)798–808. . [Online]. Available: https://www.ncbi.nlm.nih.gov/pubmed/26646466.
3. Peter MA, Bentley BJ, Mary ME, Jim C, Allan de Caen R, Farhan B, et al. Cardiopulmonary resuscitation quality: Improving cardiac resuscitation outcomes both inside and outside the hospital. Circulation 2013;128(4)417–35. . 2020/01/06 [Online]. Available: https://doi.org/10.1161/CIR.0b013e31829d8654.
4. Marquez A, Morgan R, Ross C, Berg R, Sutton R. Physiology-directed cardiopulmonary resuscitation: Advances in precision monitoring during cardiac arrest. Current Opinion in Critical Care 2018;24:1.
5. Indik JH, Conover Z, McGovern M, Silver AE, Spaite DW, Bobrow BJ, et al. Amplitude-spectral area and chest compression release velocity independently predict hospital discharge and good neurological outcome in ventricular fibrillation out-of-hospital cardiac arrest. Resuscitation 2015;92(May):122–8.
6. Indik JHI, Allen D, Shanmugasundaram M, Zuercher M, Hilwig RW, Berg RA, et al. Predictors of resuscitation outcome in a swine model of VF cardiac arrest: A comparison of VF duration, presence of acute myocardial infarction and VF waveform. Resuscitation 2009;80:1420–3.
7. Indik JH, Conover Z, McGovern M, Silver AE, Kern KB. Association of amplitude spectral area of the ventricular fibrillation waveform with survival of out-of-hospital ventricular fibrillation cardiac arrest. Journal of American College of Cardiology 2014;64(13):1362–9.
8. Nadkarni VM, Larkin GL, Peberdy MA, Carey SM, Kaye W, Mancini ME, et al. First documented rhythm and clinical outcome from in-hospital cardiac arrest among children and adults. JAMA 2006;295(1) 50–7. . [Online]. Available: https://doi.org/10.1001/jama.295.1.50.
9. Berg RA, Hilwig RW, Kern KB, Allen G. Precountershock cardiopulmonary resuscitation improves ventricular fibrillation median frequency and myocardial readiness for successful defibrillation from prolonged ventricular fibrillation: A randomized, controlled swine study. Annals of Emergency Medicine 2002;40(6):563–71.
10. Howe A, Escalona OJ, Maio RD, Massot B, Cromie NA, Darragh KM, et al. A support vector machine for predicting defibrillation outcomes from waveform metrics. Resuscitation 2014;85 (November):343–9.
11. Indik JH, Allen D, Shanmugasundaram M, Zuercher M, Hilwig RW, Berg RA, et al. Predictors of resuscitation in a swine model of ischemic and nonischemic ventricular fibrillation cardiac arrest: Superiority of amplitude spectral area and slope to predict a return of spontaneous circulation when resuscitation eff ;orts are prolonged. Society of Critical Care Medicine 2010;38(12):2352–7.

12. Indik JH, Donnerstein RL, Berg MD, Samson RA, Berg RA. Ventricular fibrillation frequency characteristics and time evolution in piglets: a developmental study. Resuscitation 2004;63:85–92.
13. Bonnes JL, Thannhauser J, Nas J, Westra SW, Rutger GMJ, Jansen MG, et al. Ventricular fibrillation waveform characteristics of the surface ECG: Impact of the left ventricular diameter and mass. Resuscitation 2017;115(March):82–9.
14. Bonnes JL, Thannhauser J, Hermans MC, Westra SW, Oostendorp TF, Meinsma G, et al. Ventricular fibrillation waveform characteristics diff ;er according to the presence of a previous myocardial infarction: A surface ECG study in ICD-patients. Resuscitation 2015;96 (August):239–45.
15. Yongqin L, Tang W. Optimizing the timing of defibrillation: The role of ventricular fibrillation waveform analysis during cardiopulmonary resuscitation. Critical care clinics 2012;28(April (2)):199–210.
16. Naim MY, Sutton RM, Friess SH, Bratinov G, Bhalala U, Kilbaugh TJ, et al. Blood pressure– and coronary perfusion pressure–targeted cardiopulmonary resuscitation improves 24-hour survival from ventricular fibrillation cardiac arrest. Critical Care Medicine 2016;44 (November (11)):1111–7.
17. Sutton RM, Friess SH, Naim MY, Lampe JW, Bratinov G, Weiland TR, et al. Patient-centric blood pressure–targeted cardiopulmonary resuscitation improves survival from cardiac arrest. American Journal of Respiratory and Critical Care Medicine 2014;190(December (11)):1255–62.
18. ECC Guidelines. Circulation 2000;102(August (1)):I-253–90.
19. *Basic Algorithms for Advanced Cardiac Life Support 2019*, Advanced Cardiovascular Life Support, January 2019.
20. Daubechies I. Ten Lectures on Wavelets. 1st ed The Society for Industrial and Applied Mathematics; 1992.
21. Bender D, Nadkarni VM, Nataraj C. A machine learning algorithm to improve patient-centric pediatric cardiopulmonary resuscitation. Informatics in Medicine Unlocked 2020;19:100339. . [Online]. Available: http://www.sciencedirect.com/science/article/pii/S2352914820300381.
22. Addison PS. The Illustrated Wavelet Transform Handbook. 2nd ed Taylor and Francis Group; 2017.
23. Daubechies I, Lu J, Wu H. Synchrosqueezed wavelet transforms: an empirical mode decomposition-like tool. Applied and Computational Harmonic Analysis 2011(July).
24. Auger F, Flandrin P. Improving the readability of time-frequency and time-scale representations by the reassignment method. IEEE Transactions on Signal Processing 199543(May).
25. Auger F, Flandrin P, Lin Y, McLaughlin S, Meignen S, Oberlin T, et al. A coherent overview of time-frequency reassignment and synchrosqueezing. IEEE Signal Processing Magazine 2013;30(6): 32–41.
26. Molinaro AM, Simon R, Pfeiffer RM. Prediction error estimation: a comparison of resampling methods. Bioinformatics 2005;21(Aug (15)):3301–7.
27. Russell SJ, Norvig P. Artificial Intelligence a Modern Approach. 3rd ed Pearson Higher Education; 2010.
28. Audet C, Dennis J. Analysis of generalized pattern searches. SIAM Journal on Optimization 2003;13(3):889–903.
29. Ruggeri L, Semeraro F, Ristagno G. Amplitude spectrum area: The "clairvoyance" during resuscitation in the era of predictive medicine. Resuscitation 2017120(Setember).
30. Hullemana M, Salcidob DD, Menegazzib JJ, Souvereinc PC, Tana HL, Bloma MT, et al. Predictive value of amplitude spectrum area of ventricular fibrillation waveform in patients with acute or previous myocardial infarction in out-of-hospital cardiac arrest. Resuscitation 2017;120(August):125–31.
31. Ristagno G, Mauri T, Cesana G, Li Y, Finzi A, Fumagalli F, et al. Amplitude spectrum area to guide defibrillation. Circulation 2014 (November).
32. Ristagnoa G, Li Y, Fumagallia F, Finzi A, Quan W. Amplitude spectrum area to guide resuscitation - a retrospective analysis during out-of-hospital cardiopulmonary resuscitation in 609 patients with ventricular fibrillation cardiac arrest. Resuscitation 2013;84(August):1697–703.
33. Young C, Bisera J, Gehman S, Snyder D, Tang W, Weil MH. Amplitude spectrum area: Measuring the probability of successful defibrillation as applied to human data. Crit Care Med 2004;32(9):356–8.
34. Wu X, Biser J, Tang W. Signal integral for optimizing the timing of defibrillation. Resuscitation 2013;84:1704–7.
35. DeLong ER, DeLong DM, Clarke-Pearson DL. Comparing the areas under two or more correlated receiver operating characteristic curves: a nonparametric approach. Biometrics 1988;44(Sep (3)):837–45.
36. Robin X, Turck N, Hainard A, Tiberti N, Lisacek F, Sanchez J, et al. pROC: an open-source package for R and S+ to analyze and compare ROC curves. BMC Bioinformatics 2011;12(1)77. . [Online]. Available: https://doi.org/10.1186/1471-2105-12-77.
37. Kaiser G. In: Stock M, editor. A friendly Guide to Wavelets. 1st ed. Massachusetts Avenue, Cambridge, MA 02139: Birkhaeuser Boston; 1994.
38. Northwestern University. Wavelets: A New Tool for Signal Analysis. 2017.
39. Daubechies I, Maes S. A nonlinear squeezing of the continuous wavelet transform based on auditory nerve models. Human Language Technologies 1996.
40. Morgan RW, Sutton RM, Karlsson M, Lautz A, Mavroudis C, Landis W, et al. Pulmonary vasodilator therapy in shock-associated cardiac arrest. American Journal of Respiratory and Critical Care Medicine 2017197:.
41. Morgan RW, Kilbaugh TJ, Shoap W, Bratinov G, Lin Y, Hsieh T, et al. A hemodynamic-directed approach to pediatric cardiopulmonary resuscitation (HD-CPR) improves survival. Resuscitation 2017;111:41–7. . [Online]. Available: https://www.ncbi.nlm.nih.gov/pubmed/27923692.
42. Sutton RM, French B, Meaney PA, Topjian AA, Parshuram CS, Edelson DP, et al. Physiologic monitoring of CPR quality during adult cardiac arrest: A propensity-matched cohort study. Resuscitation 2016;106:76–82. . [Online]. Available: https://www.ncbi.nlm.nih.gov/pubmed/27350369.
43. Salcido DD, Menegazzi JJ, Suff ;oletto BP, Logue ES, Sherman LD. Association of intramyocardial high energy phosphate concentrations with quantitative measures of the ventricular fibrillation electrocardiogram waveform. Resuscitation 2009;80(Aug (8)): 946–50.
44. Himebauch AS, Yehya N, Wang Y, McGowan FX, Mercer-Rosa L. New or persistent right ventricular systolic dysfunction is associated with worse outcomes in pediatric acute respiratory distress syndrome. Pediatric Critical Care Medicine 202021(2) [Online]. Available: https://journals.lww.com/pccmjournal/Fulltext/2020/02000/Newo r P er si st entR ightV ent r icularS y st olic.23.a s p x.